A metastable hydrogen probe beam to measure static and oscillating electric fields

L. Chérigier-Kovacic[1], C. Poggi[1], T. Guillaume[1], F. Doveil[1]

[1] *Aix-Marseille University / CNRS UMR 7345, Marseille, France*

A new diagnostic to measure directly an electric field in vacuum or in a plasma has been developed. Absolute measurements of a static electric field between two polarized metallic plates in vacuum or in the sheath between a plasma and one of the plates have been successfully performed [1]. We now address the case of oscillating fields in vacuum: measurements of a radiofrequency field (in function of injected power and frequency in the range 800-1400 MHz) compare well to simulations of our experimental process. We draw conclusions about calibration.

Experimental scheme

The diagnostic is based on the emission of the Lyman-α line by a hydrogen probe-beam in the 2s state when the beam passes through a region where an electric field is present (Electric Field Induced Lyman-α Emission). The electric field couples 2s and 2p atomic hydrogen levels, the 2s lifetime is shortened and this level decays via 2p to the ground state. For small enough values of electric field E (typically lower than about 4000 V·m^{-1} in the case of a static field), the intensity of the Lyman-α radiation, proportionnal to $\gamma^*_{2s}(E,\nu)$ the modified transition rate of 2s[2], is given by:

$$I = \beta L(\nu) E^2 \tag{1}$$

where β is a factor including initial beam density and transparency of the whole detection device, ν is the frequency of the electric field and $L(\nu)$ is a Lorentzian function centered on the frequency corresponding to Lamb-shift (energy difference between 2s and 2p). By measuring the intensity of the Lyman-α radiation, it is therefore possible to determine the magnitude of the field in a defined region.

Fig. 1 shows a scheme of the experimental setup. A two-plate assembly is used to generate an electric field: a static voltage or radiofrequency power supply, both controlled by a computer, are connected to the upper plate while the lower one is grounded. A mestastable hydrogen probe-beam passes between the plates, where the electric field is measured. The Lyman-α emission is detected by a VUV-photmultiplier, perpendicularly to the beam. Either the beam or the electric field are pulsed and a lock-in amplifier is used to improve the signal/noise ration. A small probe (antenna) can also be placed between the plates to detect the local RF electric signal. A more

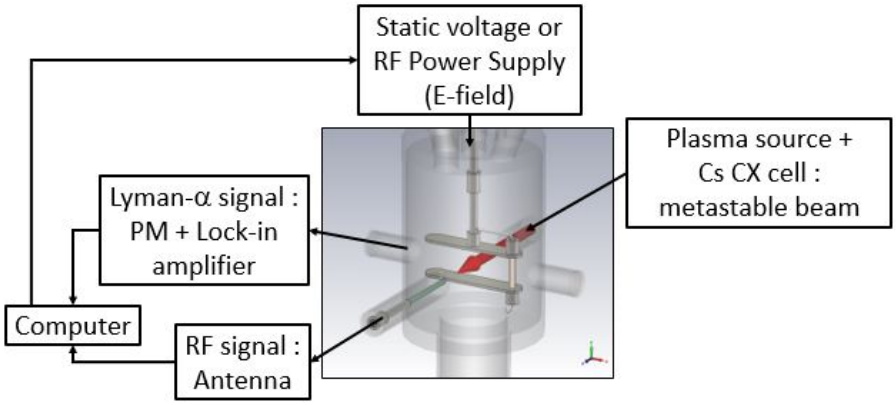

Figure 1: *Experimental scheme*

detailed description of performances, experimental and physical principles of the diagnostic can be found in previous publications [1].

Numerical simulation

The CST Studio Suite software [3] is used to create a 3D model of the test chamber and to solve Maxwell equations in vacuum, when a static or RF voltage is applied between the electrodes. First, the field map is computed. Then the Lyman-α signal between the plates is calculated: it is proportionnal to the number of metastable atoms in the intersection of the beam with the volume viewed by the photomultiplier. Fig. 2 displays the computed electric field magnitude along the beam path (z-axis) over a large range of frequencies. The white vertical dashed lines indicate the edges of the plates, arbitrarly centered on zero. Fig. 2 exhibits a finite number of strong resonant frequencies in the vessel (in yellow/white). It shows that the beam is exposed to an electric field all along its path from the edge of the test vessel to the diagnosed volume between the plates. This induces the exponential decay, governed by $\gamma^*_{2s}(E(\vec{r}),\nu)$, of metastable atoms before the diagnosed volume. This is the cause of a "geometrical saturation" of the Lyman-α signal between the plates, also observed in a static field case. It also shows that the amplitude of the field encountered by the beam is not the same for all frequencies. Signal amplitudes at different frequencies can therefore not be directly comparated.

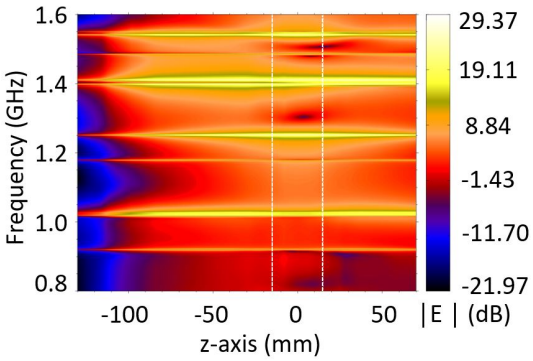

Figure 2: *CST-Computed electric field magnitude in function of frequency along z*

The calculated Lyman-α signal intensity is displayed in Fig. 3 in the case of a static voltage ($\nu = 0$) applied between the plates, along with a fit by the function $f(V) = AV^2 e^{-BV^2}$, also used to fit our experimental data. This function accounts for the geometrical saturation previously described. Saturation occurs for voltages greater than about 200 V which, for 5cm-spaced electrodes, gives $E > 4000\ \mathrm{V{\cdot}m^{-1}}$).

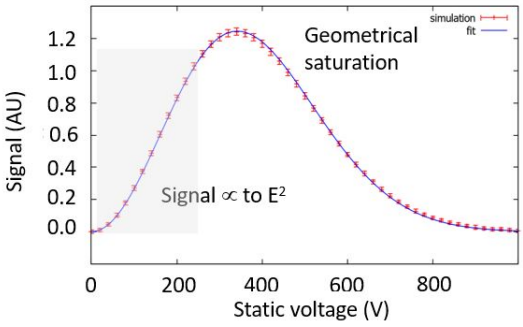

Figure 3: *Calculated Lyman-α signal*

Experimental results

The signal measured at center and edge of the vessel by a 2 cm-bare wire antenna in function of frequency of oscillating voltage applied between the plates is displayed in Fig. 4. Peaks at the same resonant frequencies as those calculated are clearly observed. Three peaks (1.026 GHz, 1.252 GHz and 1.404 GHz) also coincide well with Lyman-α (Fig. 4, right scale) and calculated data. In both simulation and experimental results, these peaks are robust under small modifications of vessel geometry (position of metallic elements in the vessel).

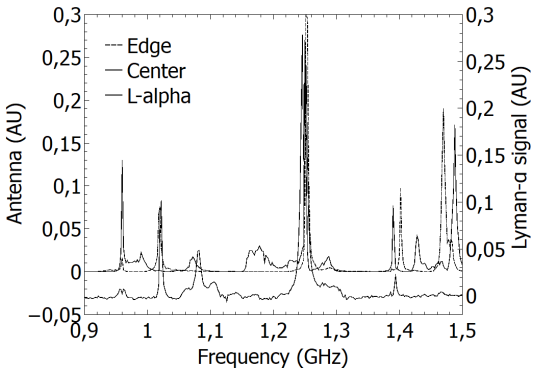

Figure 4: *E-field spectra in vessel measured by Lyman-α emission or antenna*

A calibration method based on the measurement of the Lyman-α signal resulting from the superposition of both static and oscillating E-fields is proposed. Fig. 5 (main) shows raw Lyman-α signal at 1.256 GHz, at various values of injected power from 0 mW (static field case) to 1000 mW, in function of square of static electric field magnitude. All curves show the same linear dependance for non-saturating values of the static field. We make the simplifying assumption that γ^*_{2s} is the sum of transition rates when static and oscillating fields are superposed. In the non-saturating range of variables P and E_0, the total signal $S(E_0, P)$ is thus:

$$S(E_0, P) = \beta L(0) E_0^2 + \beta L(\nu) E_{\mathrm{osc}}^2(P) \qquad (2)$$

Factor β is deduced from $S(E_0, 0)$ (lowest curve in Fig. 5-main). Then we calculate the oscillating field amplitude from Eq. (2). The result is displayed on the smallest graph of Fig. 5. We can see that values as small as 1V/cm can be detected. As long as the signal is not saturated, E_{osc} varies like $\sqrt{P}$. Otherwise, the field is underestimated because of saturation.

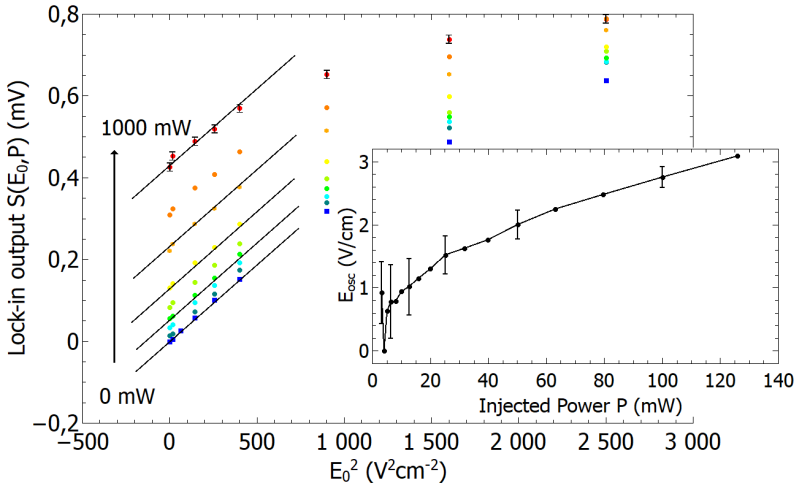

Figure 5: *Raw Lock-in output signal data in function of static electric field at different injected powers and calibrated oscillating electric field*

Conclusion

E-FILE (Electric Field Induced Lyman-α Emission) is a diagnostic for the measurement of a static or oscillating local electric field, based on the emission of Lyman-α line by a metastable hydrogen beam subject to an electric field. Measurement of the Lyman-α signal in function of frequency of an oscillating voltage applied between two plates exhibits resonant frequencies of the vessel in vacuum. This is in agreement with the results of numerical calculations. In order to calibrate the whole spectrum, measurements with superposed static and oscillating electric fields at various amplitudes/injected powers have to be performed. It has been done for one frequency (1.252 GHz) assuming, as a first approximation, that transition rates for static and oscillating fields can be added. This gives a detection limit of about 1 V/cm. A calculation of the actual transition rate for superposed fields will be done. Only preliminary experiments have been performed in a plasma so far (not presented here because this work is still in progress).

Acknowledgements

We thank G. Demesy, P. Sabouroux and M. Dubois of the Fresnel Institute (AMU) for fruitful discussions and for technical support with CST. CP benefited from an Erasmus exchange grant via the European Erasmus+ Programme 2014-2020.

References

[1] C. Poggi *et al.*, Plasma Sci. Technol. **20**, 074001 (2018) ; L. Chérigier-Kovacic *et al.*, Review of Scientific Instruments **86**, 063504 (2015)

[2] W. E. Lamb, Jr. and R. C. Retherford, Phys. Rev. **79**, 549 (1950)

[3] CST / Dassault Systemes. 2018. Computer Science Technology. [ONLINE] Available at: https://www.cst.com. [Accessed 28 June 2018]